Supplement of Atmos. Chem. Phys., 23, 5815–5834, 2023
https://doi.org/10.5194/acp-23-5815-2023-supplement
© Author(s) 2023. CC BY 4.0 License.

Atmospheric Chemistry and Physics
Open Access

Supplement of

A new insight into the vertical differences in NO_2 heterogeneous reaction to produce HONO over inland and marginal seas

Chengzhi Xing et al.

Correspondence to: Cheng Liu (chliu81@ustc.edu.cn) and Keding Lu (k.lu@pku.edu.cn)

The copyright of individual parts of the supplement might differ from the article licence.

Section S1: The algorithm of vertical profile retrieval

The maximum a posteriori state vector $\mathbf{x}$ is determined by minimizing the following cost function χ^2.

$$\chi^2 = (\mathbf{y} - F(\mathbf{x},\mathbf{b}))^T \mathbf{S}_\varepsilon^{-1} (\mathbf{y} - F(\mathbf{x},\mathbf{b})) + (\mathbf{x} - \mathbf{x}_a)^T \mathbf{S}_a^{-1} (\mathbf{x} - \mathbf{x}_a) \quad (1)$$

Here, $F(\mathbf{x},\mathbf{b})$ is the forward model, which describes the measured DSCDs $\mathbf{y}$ as a function of the retrieval state vector $\mathbf{x}$ (i.e., aerosol and trace gas vertical profiles) and the meteorological parameters $\mathbf{b}$ (e.g., atmospheric pressure and temperature profiles); $\mathbf{x}_a$ denotes the a priori vector that serves as an additional constraint; $\mathbf{S}_\varepsilon$ and $\mathbf{S}_a$ are the covariance matrices of $\mathbf{y}$ and $\mathbf{x}_a$, respectively. The retrieval of vertical profiles of aerosols and trace gases were classified into two steps (Figure S3). First, we retrieved vertical aerosol profiles based on a series of retrieved O_4 DSCDs at different elevation angles. Second, the retrieved aerosol extinction profiles were utilized as the input parameters to the radiative transfer model to retrieve NO_2 and HONO vertical profiles. Each scanning sequence of DSCD results (~5.5 min) correspond to one retrieved vertical profile information. In this study, we separated the atmosphere into 19 layers from 0 to 3.8 km with a vertical resolution of 0.2 km. Given the low sensitivity of MAX-DOAS measurements to high altitude and low concentration of pollutants above 3.0 km, we only displayed the vertical profiles below 3.0 km in this work.

Section S2: The criteria of the identification of fresh plumes

The fresh plumes were selected using the following criteria: (a) $[NO_x]$>40 ppb, (b) NO/NO_x>0.85, (c) good correlation performing between HONO and NO_x (R>0.90), (d) short duration of plumes (<=2.0 h), and (e) 70^o<SZA<75^o.

MAX-DOAS performed based on the collected solar scattering spectrum to retrieve aerosol, NO_2 and HONO. In general, we believed that the retrieved MAX-DOAS data was reliable, when SZA was not large than 75^o. In order to reduce the influence of fast photolysis of HONO and NO_2, we usually selected data with 70^o<SZA<75^o to calculated $HONO/NO_x$ ratios from direct emission. In this condition, the photolysis rate of NO_2 was not large than 0.25×10^{-3} s^{-1}. The slopes of HONO to NOx in selected plumes were considered as the emission ratios.

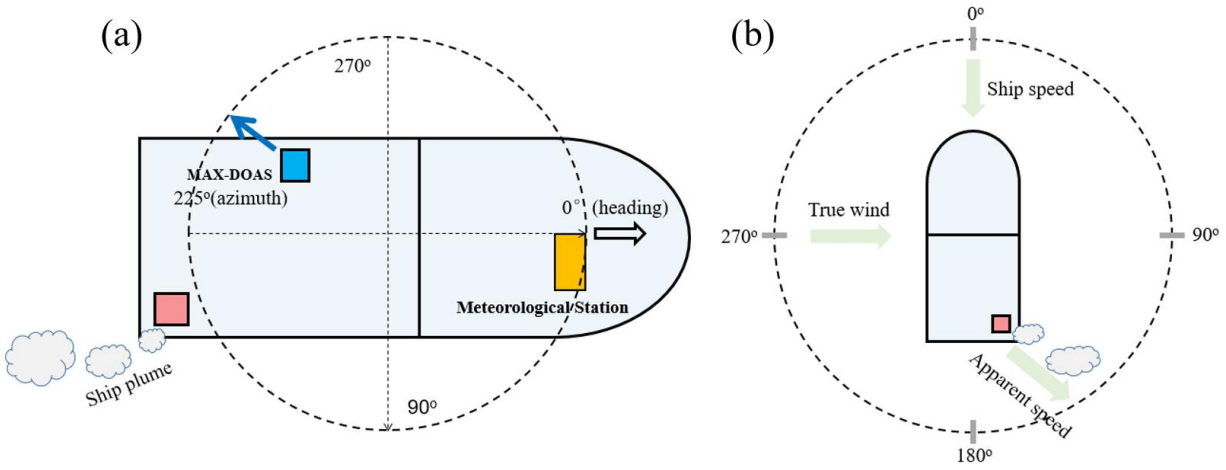

Figure S1. (a) Illustration of the MAX-DOAS setup location on the measurement ship. The red rectangle indicates the ship's exhaust. The blue rectangle represents the MAX-DOAS instrument. The blue rectangle represents the meteorological station. (b) The apparent speed and direction of plume.

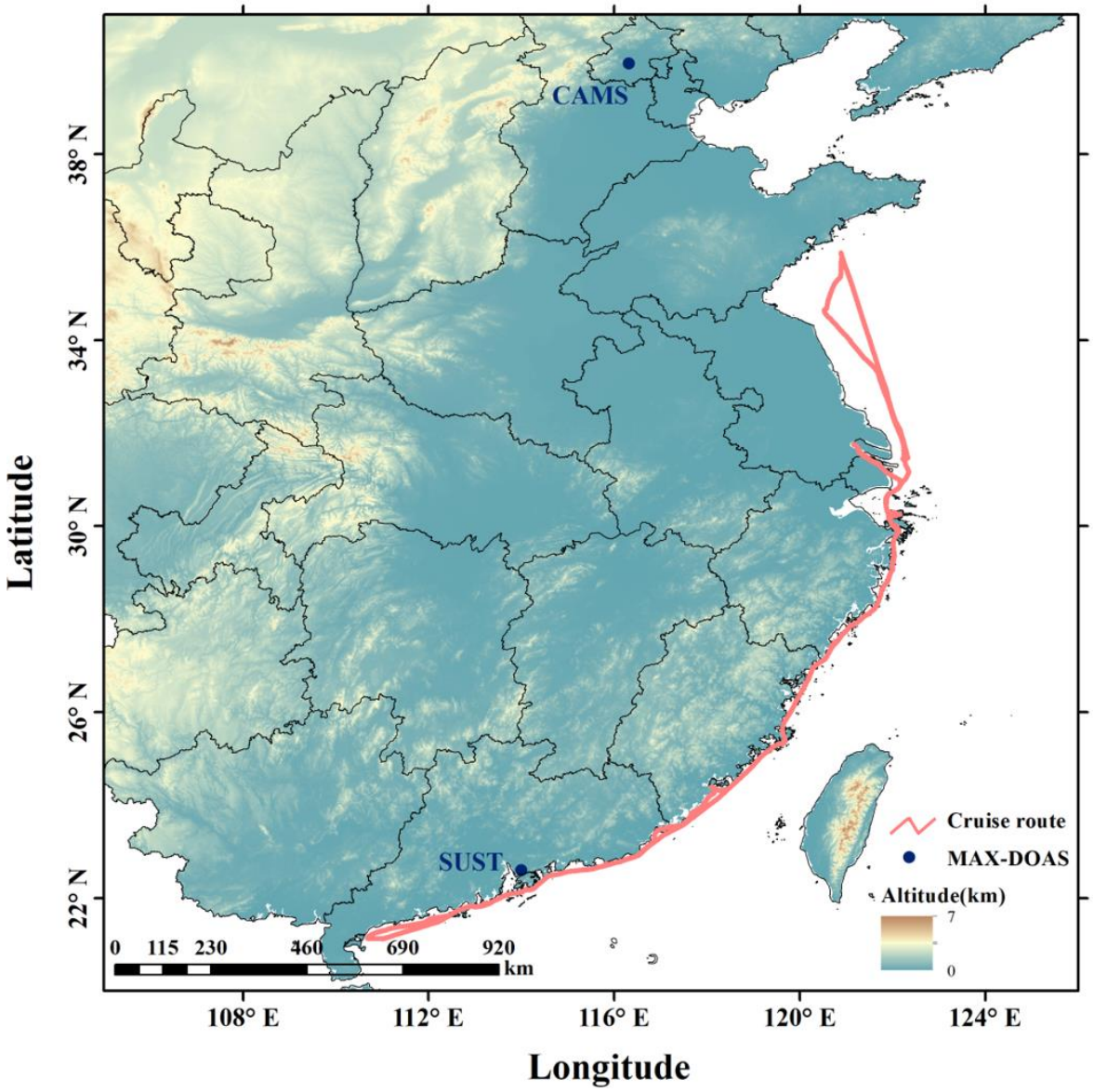

Figure S2. Cruise route and the location of two MAX-DOAS stations (CAMS and SUST).

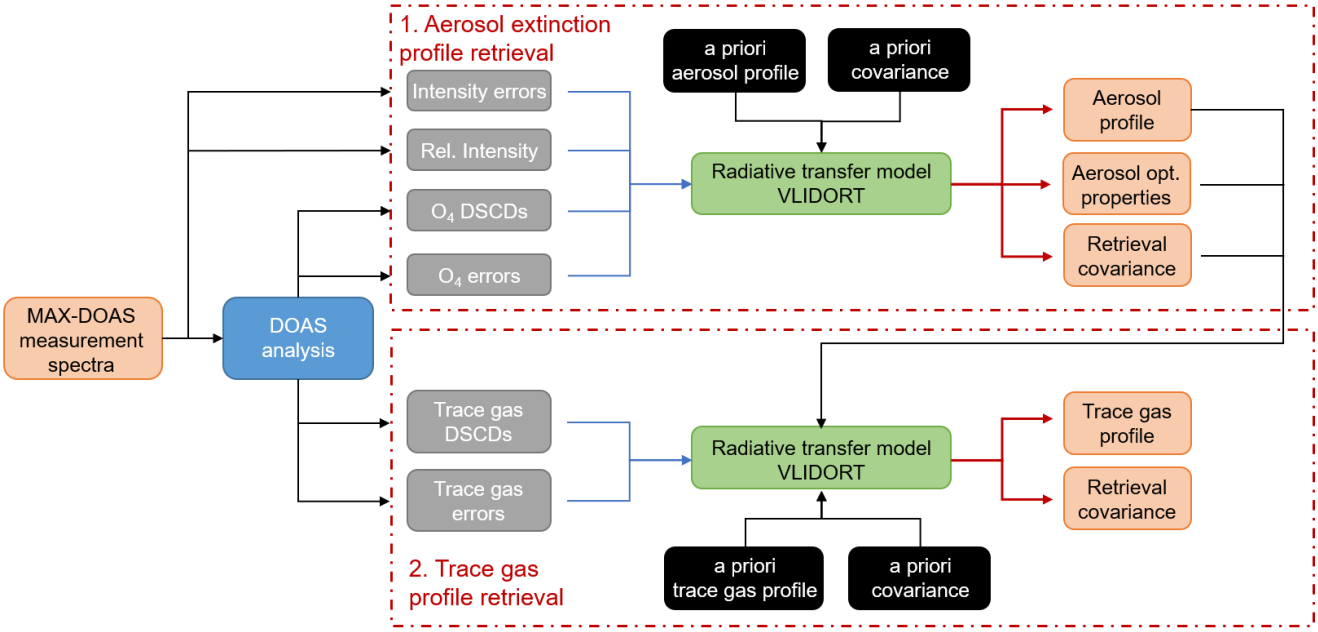

Figure S3. Flowchart of the aerosol and trace gas retrieval algorithm. The dashed-lined red boxes denote the retrieval steps: aerosol and trace gas profile retrieval.

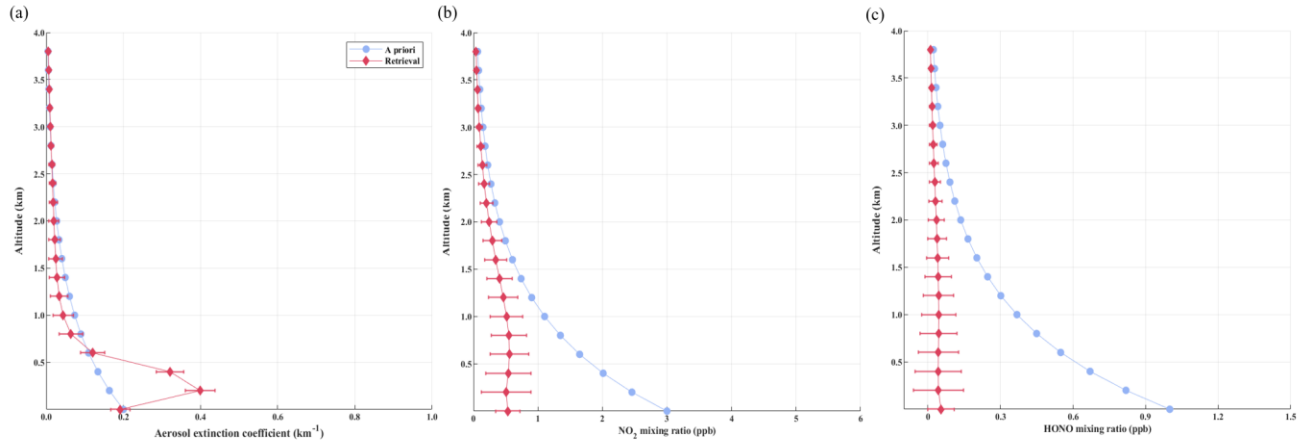

Figure S4. An example of the a priori and retrieved profiles from MAX-DOAS measurements in ship-based campaign (May 1, 2019 at 08:02 LT) for (a) aerosol extinction, (b) NO_2, and (c) HONO.

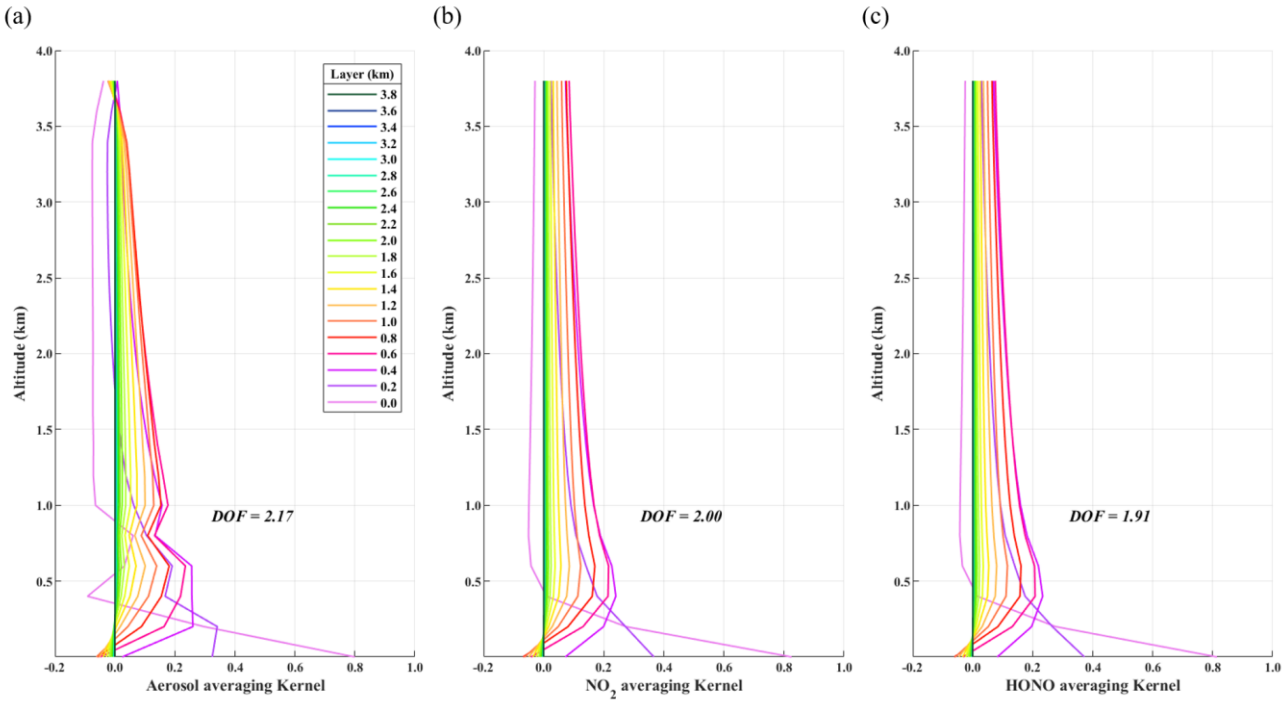

Figure S5. An example of averaging kernel results from MAX-DOAS measurements in ship-based campaign (May 1, 2019 at 08:02 LT) for (a) aerosol extinction, (b) NO_2, and (c) HONO.

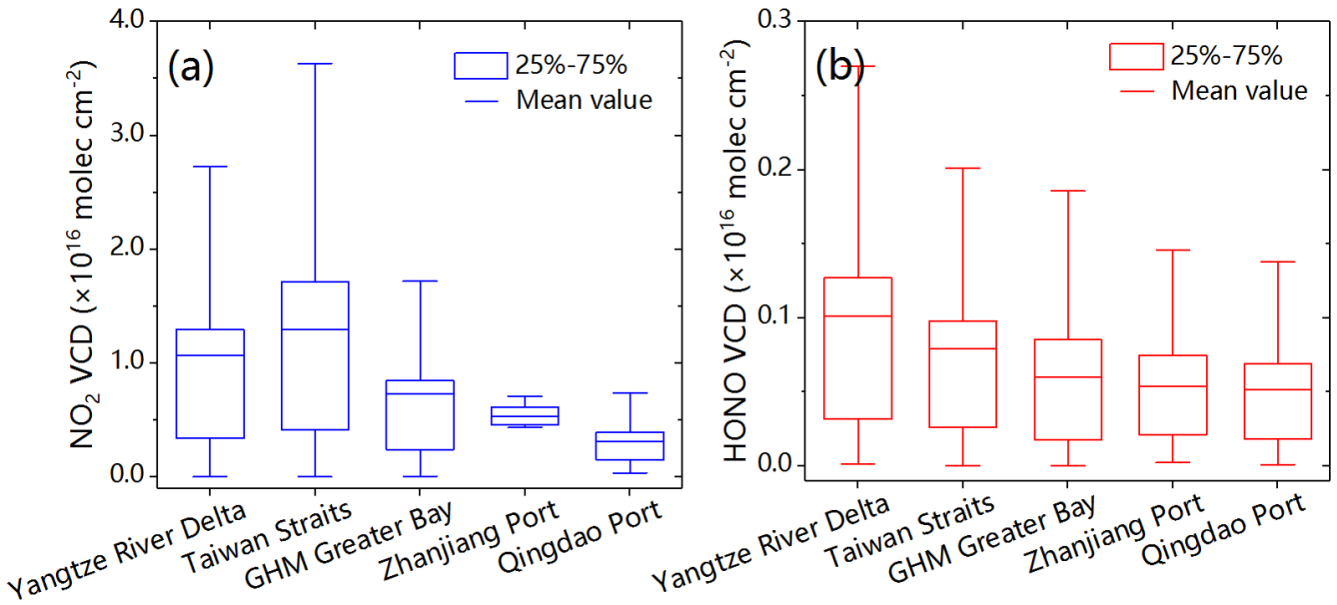

Figure S6. The VCD distribution of (a) NO_2 and (b) HONO for five high-level emission sources (i.e., the coastal areas of Yangtze River Delta, Taiwan straits, Guangzhou-Hong Kong-Macao Greater Bay areas, Zhanjiang Port, and Qingdao port) along the cruise.

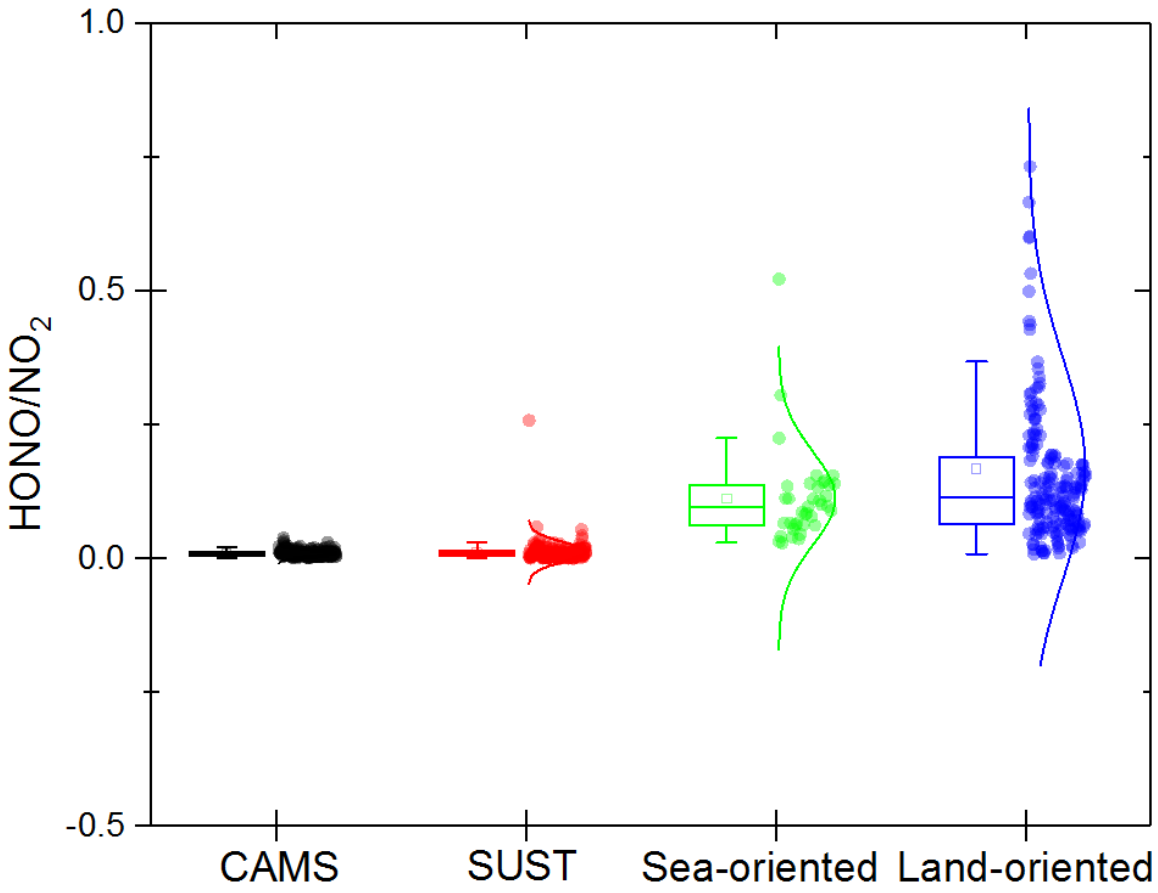

Figure S7. $HONO/NO_2$ ratios in CAMS, SUST and the cruise.

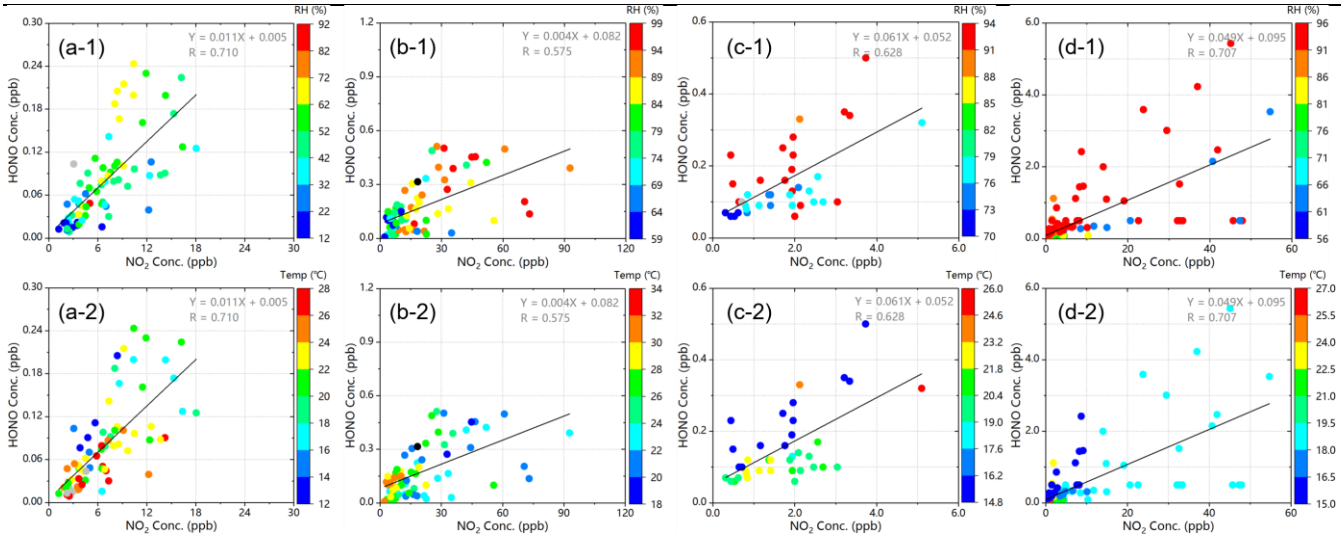

Figure S8. Scatter plots of HONO concentration vs. NO_2 concentration coloured by (1) relative humidity (RH) and (2) temperature in (a) CAMS, (b) SUST, and ship-based measurements of (c) sea-oriented and (d) land-oriented under static weather condition.

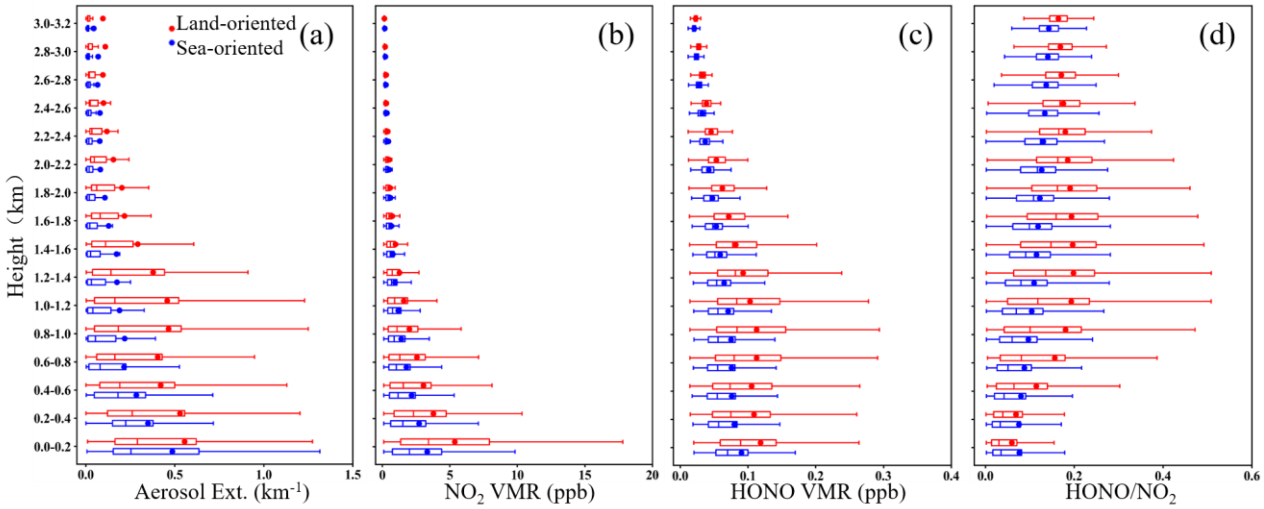

Figure S9. Vertical profiles of (a) aerosol extinction, (b) NO_2, (c) HONO, and HONO/NO_2 ratios during the cruise observation.

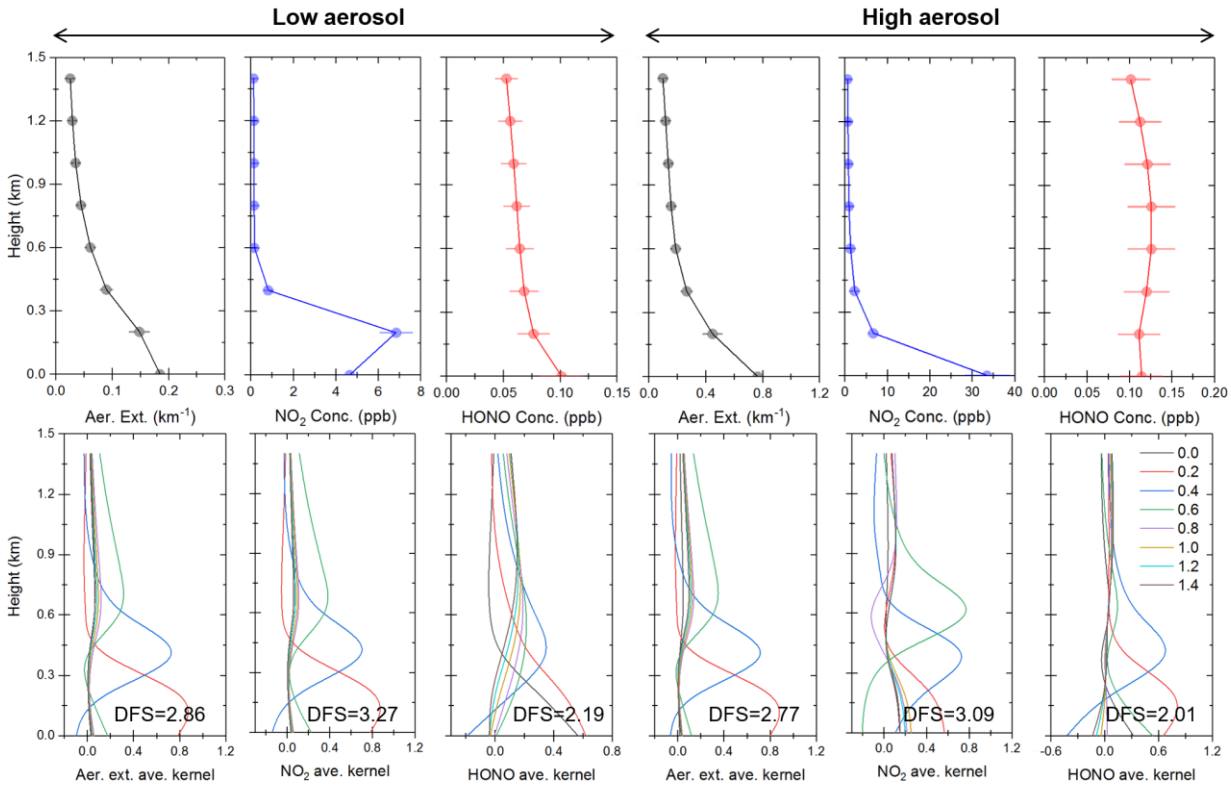

Figure S10. The top row presented the vertical profiles and errors of aerosol, NO_2 and HONO under low aerosol and high aerosol conditions. The bottom row showed the corresponding retrieved averaging kernels.

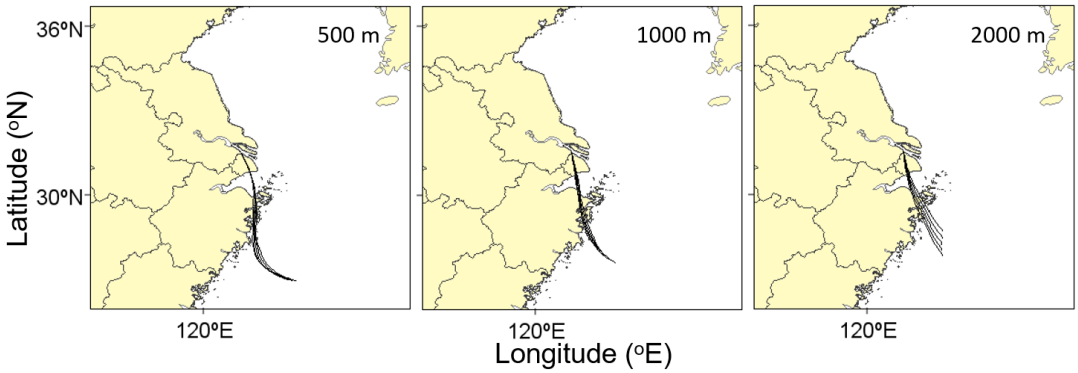

Figure S11. Daily 24-h backward trajectories of air masses at (a) 500 m, (b) 1000 m, and (c) 2000 m on 20 April 2018, respectively.

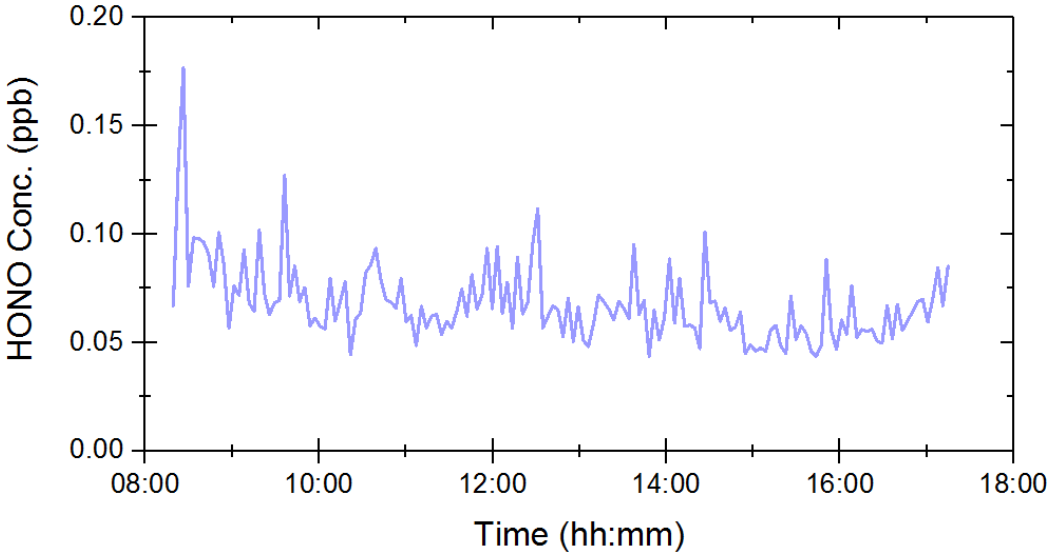

Figure S12. Time series of HONO at bottom layer on 20 April 2018.

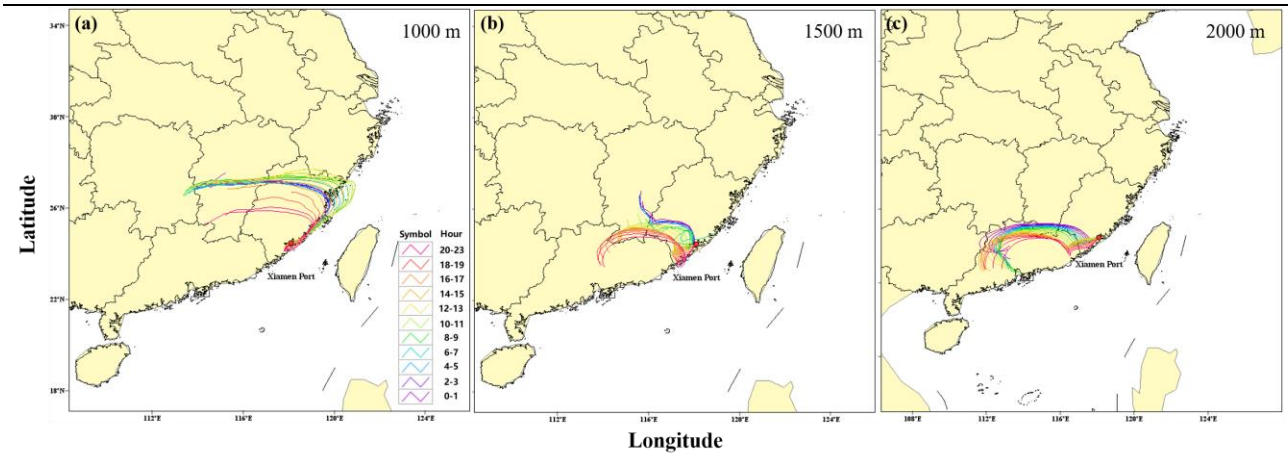

Figure S13. Daily 72-h backward trajectories of air masses in Xiamen port at (a) 1000 m, (b) 1500 m, and (c) 2000 m on 28 April 2018, respectively.

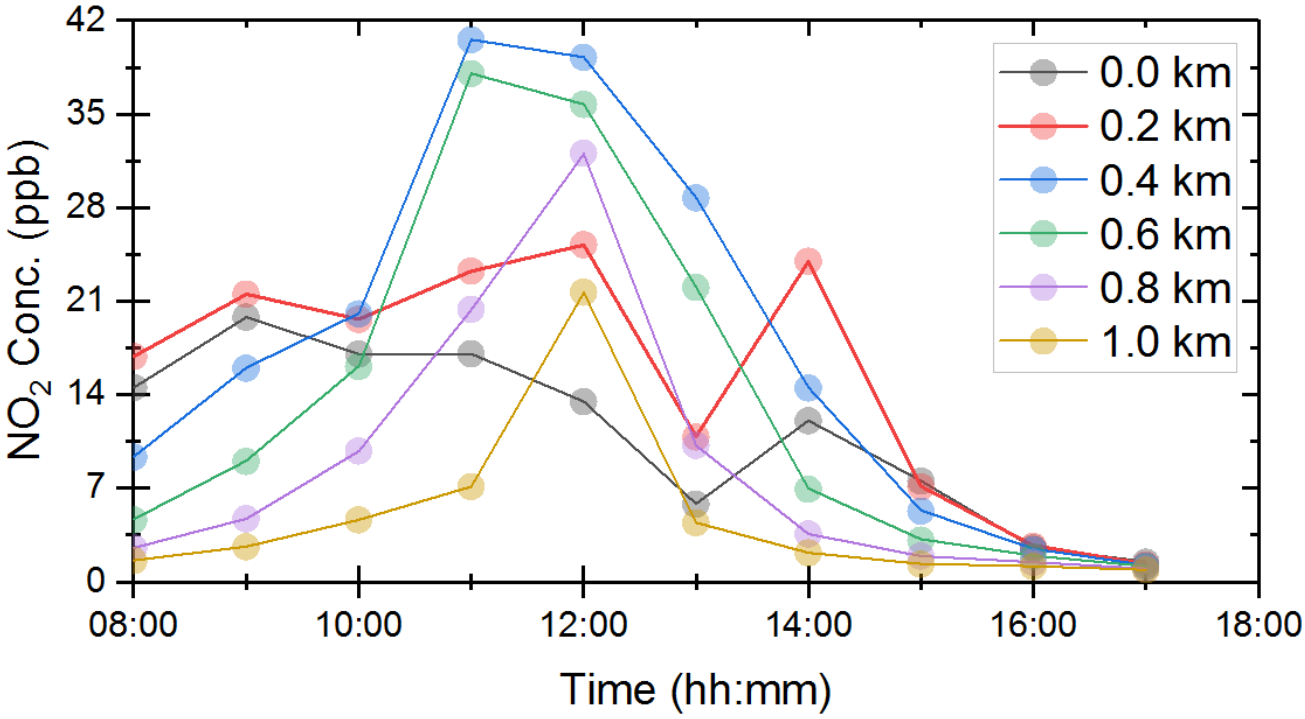

Figure S14. Time series of NO_2 at 6 layers on 03 May 2018.